Corrosion Science 51 (2009) 841–849

Contents lists available at ScienceDirect

Corrosion Science

journal homepage: www.elsevier.com/locate/corsci

Corrosion behaviour of silicon–carbide-particle reinforced AZ92 magnesium alloy

A. Pardo [a,*], S. Merino [b], M.C. Merino [a], I. Barroso [a], M. Mohedano [a], R. Arrabal [a], F. Viejo [a]

[a] Departamento de Ciencia de Materiales, Facultad de Químicas, Universidad Complutense, 28040 Madrid, Spain
[b] Departamento de Tecnología Industrial, Universidad Alfonso X El Sabio, 28691, Villanueva de la Cañada, Madrid, Spain

ARTICLE INFO

Article history:
Received 24 October 2008
Accepted 28 January 2009
Available online 6 February 2009

Keywords:
A. Magnesium
A. Metal matrix composites
B. Polarization
B. Atmospheric corrosion
B. Weight loss

ABSTRACT

The corrosion behaviour of silicon–carbide-particle (SiCp) reinforced AZ92 magnesium alloy manufactured by a powder metallurgy process was evaluated in 3.5 wt.% NaCl solution, neutral salt fog (ASTM B 117) and high relative humidity (98% RH, 50 °C) environments. The findings revealed severe corrosion of AZ92/SiC/0-10p materials in salt fog environment with formation of corrosion products consisting of $Mg(OH)_2$ and $(Mg,Al)_x(OH)_y$. The addition of SiCp increased the corrosion rate and promoted cracking and spalling of the corrosion layer for increasing exposure times. Composite materials revealed higher corrosion resistance in high humidity atmosphere with almost no influence of SiCp on the corrosion behaviour.

1. Introduction

Owing to the high specific strength of magnesium alloys there is an increasing interest on their use as structural materials in aerospace and automotive industries for applications where weigh reduction is a critical factor [1,2].

The low density of magnesium alloys combined with the incorporation of a ceramic reinforcement results in lightweight composites with exceptional strength and stiffness to weight ratios [3]. Thus, magnesium metal matrix composites (MMCs) are excellent candidates for certain applications where the performance of conventional unreinforced magnesium alloys is insufficient.

Among the available techniques for the manufacture of MMCs, powder metallurgy (P/M) technique provides a number of advantages, such as low manufacturing temperature and uniform distribution of the reinforcement [4,5]. Most of the published studies on magnesium MMCs refer to their mechanical properties and nucleation phenomena, which depend on the manufacture process, magnesium matrix composition and type of reinforcement [6–8]. However, application of magnesium MMCs is still at the development stage due to various economic and technical reasons, in particular, the relatively poor corrosion resistance of magnesium under aggressive environments [9].

Magnesium materials are susceptible to surface degradation when exposed to moisture or saline environments. Under such conditions, magnesium metal rapidly forms a corrosion layer on its surface, which commonly consists of brucite ($Mg(OH)_2$), hydromagnesite ($Mg_5(CO_3)_4$) or nesquehonite ($MgCO_3{\cdot}3H_2O$) with a relatively low protective effect [10,11]. Additionally, magnesium and magnesium alloys reveal a very active behaviour in the sea water galvanic series. Therefore, corrosion behaviour of magnesium alloys is greatly influenced by the presence of alloying elements, which may induce galvanic couples with the magnesium matrix. For instance, it is known that in case of magnesium-aluminium alloys, Mn–Al intermetallic compounds generally produce galvanic acceleration of the corrosion process [9].

The vast majority of corrosion studies on magnesium and magnesium matrix composites are based on electrochemical or physical measurements [12–15], whereas gravimetric measurements in salt fog and high humidity atmospheres are relatively scarce, despite the fact that they are very effective methods to evaluate the corrosion behaviour of metallic materials [16–20].

In the present study, the influence of SiCp proportion on the corrosion behaviour of AZ92/SiCp magnesium matrix composites, obtained by powder metallurgy route, was evaluated in saline and humidity environments by electrochemical and gravimetric measurements.

2. Experimental

2.1. Test materials

Powder of AZ92 magnesium-aluminium alloy (9% Al, 2% Zn, 0.5% Mn, bal Mg (wt.%)) of less than 100 μm in size and SiC particles of an average size of 5 μm were milled in a high speed impeller at 200 rpm for 2 h. The milled powders were cold compacted under an isostatic pressure of 220 MPa for 5 min. The resulting compacts of 40 mm in diameter were extruded at 325 °C employing and extrusion ratio of 18:1. The amount of SiC particles varied from 5

* Corresponding author. Tel.: +34 1 3944348; fax: +34 1 3944357.
E-mail address: anpardo@quim.ucm.es (A. Pardo).

0010-938X/$ - see front matter © 2009 Elsevier Ltd. All rights reserved.
doi:10.1016/j.corsci.2009.01.024

to 10% vol. (AZ92/SiC/5p, AZ92/SiC/10p). Unreinforced AZ92 magnesium alloy was used as the reference material.

2.2. Surface preparation and characterization

For metallographic characterization, specimens were prepared using successive grades of SiC paper, from P120 to P2000, followed by finishing with 0.1 μm diamond paste and immersion for 3 s in Nital etching reagent (5 ml HNO_3 + 95 ml ethanol) in order to reveal the general microstructure of the materials. Prior to corrosion tests, the surfaces of the specimens were ground to a P1200 grit SiC finish using water as lubricant, degreased with isopropyl alcohol in an ultrasonic bath and dried in warm air.

2.3. Surface hardness

Surface hardness was measured applying a load of 5 kg for 20 s by using an AKASHI AVK-AII Vickers hardness machine. Cited values are the average of ten measurements.

2.4. Electrochemical measurements

DC electrochemical measurements were performed using specimens of working area 0.30 cm^2 immersed in 3.5 wt.% NaCl at room temperature (22 ± 1 °C). An AUTOLAB model PGSTAT 30 potentiostat connected to a three-electrode cell was used for the electrochemical measurements; the working electrode was the test material, the counter electrode was graphite and the reference electrode was Ag/AgCl (SSE) with a potential of 0.197 V with respect to the standard hydrogen electrode. Solution concentration inside the reference electrode compartment was KCl 3M. Polarization measurements were carried out at a scan rate of 0.3 mV/s, from −100 mV to +400 mV with respect to the corrosion potential (E_{corr}). The anodic corrosion current was limited to 5 mA cm^{-2}.

2.5. Gravimetric measurements

Gravimetric measurements were performed using specimens with an exposed area of ~10 cm^2. Specimens were weighed before and after the tests using a Sartorius BP 211D scale with an accuracy of 0.00001 g. Corrosion rate was calculated from the mass losses per unit of surface area according to the expression $(M_i - M_f)/A$, where M_i is the initial mass, M_f the final mass and A the exposed surface area. In all cases, the tests were performed in duplicate to guarantee the reliability of the results.

The salt spray tests were performed in a CCl cabinet with the specimens hung with a nylon thread and exposed to a 5 wt.% NaCl spray (pH 6.5–7.2) during 504 h (21 days). As recommended by ASTM B 117 standard, atomized air pressure of the saline solution was maintained in the range 69–172 kN m^{-2} and the temperature inside the cabinet at 35 ± 1 °C. At the end of the tests, the specimens were washed with water below 38 °C, to remove saline deposits, dried in hot air and weighed.

The high relative humidity tests consisted of 24 h cycles performed in a saturated water vapour at 98% RH and 50 ± 1 °C during 672 h (28 days) simulated by a humidity condensation cabinet CCK 300 (Dycometal). The temperature and the humidity were verified using digitals thermometer and hygrometer. At the end of the tests, the specimens were rinsed with deionized water, dried in warm air and weighed again.

2.6. Characterization of corrosion products

After the tests, magnesium composite materials were examined by scanning electron microscopy (SEM) using a JEOL JSM-6400 microscope equipped with Oxford Link energy-dispersive X-ray (EDX) microanalysis hardware in order to study the morphology and evolution of corrosion products formed on the surface of the materials. The phase composition of the corrosion layer was examined by low-angle X-ray diffraction (XRD) studies using a Philips ΧPert diffractometer ($K_\alpha Cu$ = 1.54056 Å).

3. Results and discussion

3.1. Microstructure

The scanning electron micrograph of the unreinforced AZ92 magnesium alloy revealed $Mg_{17}Al_{12}$ and Al_8Mn_5 intermetallic compounds aligned with the extrusion direction [21]. AZ92/SiCp composite materials revealed the same constituents and uniformly distributed SiCp particles, with the longest axis aligned with the extrusion direction. In all cases the degree of porosity was relatively low (Fig. 1). XRD measurements confirmed the presence of the previous phases (Fig. 2).

3.2. Surface hardness

The addition of SiCp up to 10% vol. slightly decreased the surface hardness of the AZ92 magnesium alloy (Fig. 3). This may be explained by the influence of the SiCp on the texture of this type of materials. Thus, for similar magnesium composites, Garcés et al. [22] found that the addition of SiCp to magnesium alloys developed a fibre texture with the $10\bar{1}0$ planes perpendicular to the extrusion direction that determined the mechanical behaviour of these materials [7]. Other properties like the wear resistance, out of the scope of the present study, may be improved by the incorporation of SiCp.

3.3. Electrochemical results

Fig. 4 depicts the polarization curves of studied materials after 1 h of immersion in 3.5 wt.% NaCl solution at room temperature. The addition of SiCp slightly shifted the polarization curves towards greater corrosion current densities and more active corrosion potentials (E_{corr}). The corrosion rate (CR) increased from 4.2×10^{-2} to 5.6×10^{-2} mg cm^{-2} h^{-1} and the polarization resistance (Rp) decreased by one order of magnitude (Table 1). The SiC is an insulator and is not expected to have any galvanic interaction with the AZ92 matrix. However, it was likely that the reinforcement increased the corrosion rate due to the presence of Mg matrix/SiCp interfaces breaking the continuity of the Mg matrix and creating preferential locations for corrosion attack.

3.4. Gravimetric results

Fig. 5 discloses the mass gain versus time of AZ92, AZ92/SiC/5p and AZ92/SiC/10p materials exposed to salt spray for 504 h (21 days). Mass gain was associated with the formation of corrosion products with white colour, possibly, magnesium oxides and/or hydroxides due to the high reactivity of magnesium in chloride-containing environments [9]. At the initial stages, the unreinforced AZ92 magnesium alloy revealed lower mass gain compared with the magnesium MMCs. This was indicative of the detrimental effect of SiCp addition on the corrosion performance in salt spray, which was possibly manifested by preferential nucleation and growth of corrosion products at the matrix/SiCp interfaces [23,24]. After exposure for 300 h, the corrosion rate of AZ92 magnesium alloy increased, whereas AZ92/SiCp composites revealed mass losses. For the latter, the fast growth of the corrosion layer during the first 170 h possibly led to stresses and the subsequent

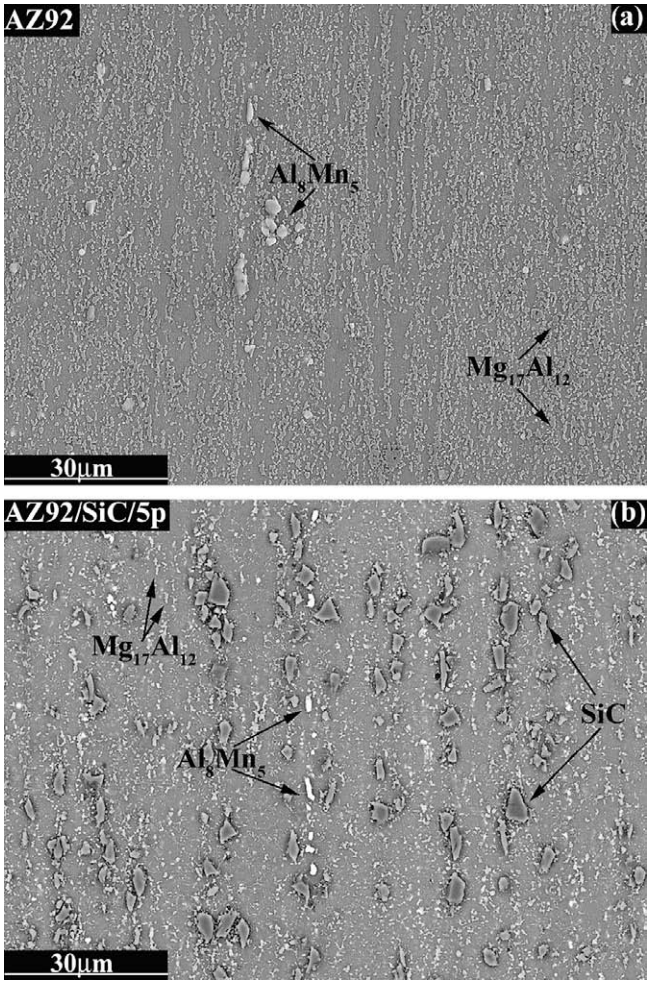

Fig. 1. Backscattered electron micrographs of AZ92 and AZ92/SiC/5p materials.

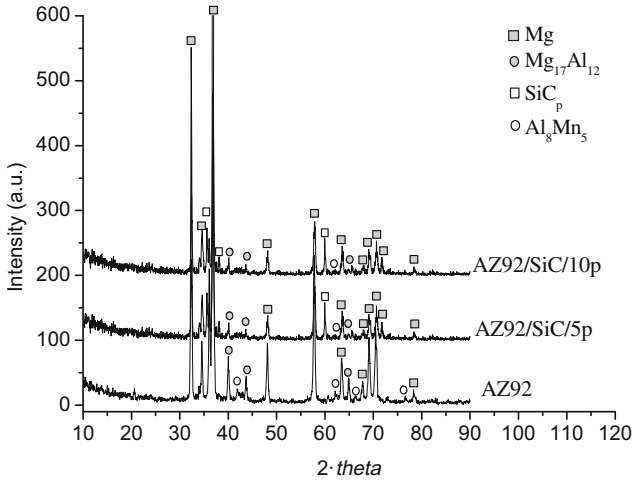

Fig. 2. XRD patterns of as-received materials.

cracking and spalling of this layer, which was more evident for a higher fraction of particulate reinforcement.

Fig. 6 discloses the mass gain versus time of tested materials exposed to 98% RH at 50 ± 1 °C for 672 h (28 days). All materials revealed high corrosion resistance with mass gain values lower than those observed in salt spray. The corrosion behaviour of

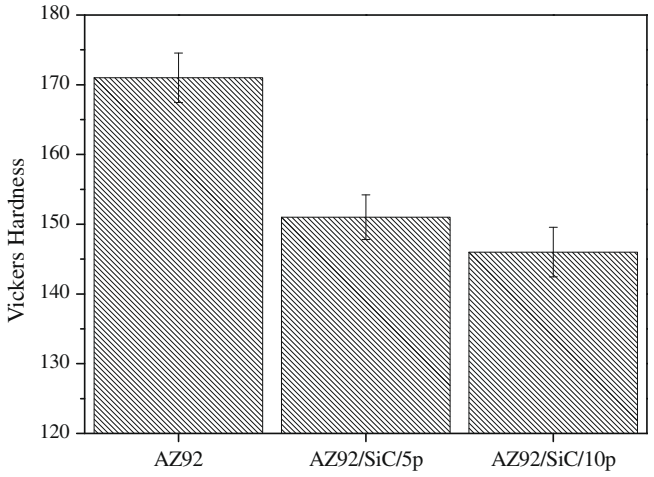

Fig. 3. Effect of SiCp addition on the surface hardness of tested materials.

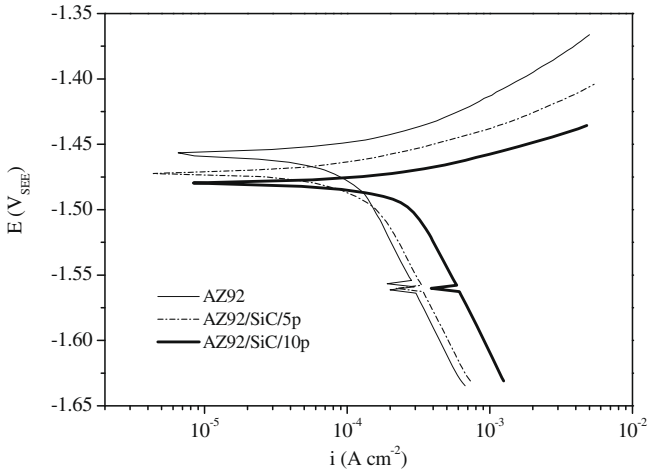

Fig. 4. Polarization curves of tested materials after immersion in 3.5 wt.% NaCl for 1 h at room temperature.

Table 1
Corrosion potential, polarization resistance and corrosion rate of tested materials after immersion in 3.5 wt.% NaCl for 1 h.

Material	E_{corr} (V/SSE)	Rp (Ω cm^2)	CR (mg cm^{-2} h^{-1})
AZ92	−1.457	142	4.2×10^{-2}
AZ92/SiC/5p	−1.472	161	4.4×10^{-2}
AZ92/SiC/10p	−1.480	50	5.6×10^{-2}

AZ92/SiCp composite materials was very similar to that of unreinforced AZ92 magnesium alloy, indicating the minor influence of SiCp on the corrosion susceptibility of these materials in high humidity atmosphere.

Table 2 shows the kinetic laws calculated from all gravimetric measurements using a linear expression ($y = b \cdot t$; y: mass gain; t: time) for exposure times where the mass gain followed a linear trend. The addition of 5 and 10% vol. SiCp increased the corrosion rate by ~4 and 5 times during the first 7 days in salt spray, respectively. For increasing exposure times, AZ92/SiC/5p and AZ92/SiC/10p composite materials revealed mass losses in the range of 3.7×10^{-4} and 6.5×10^{-4} mg cm^2 h^{-1}, respectively. This was possibly related to the cracking and spalling of the corrosion layer. On the other hand, the corrosion rates of all materials in high humidity atmosphere followed a linear trend during the entire duration of the test and were lower than in salt fog by two-three

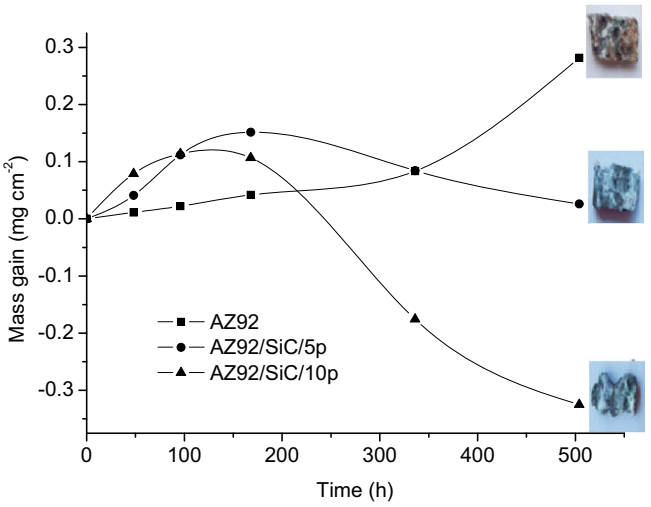

Fig. 5. Mass gain vs. immersion time for the materials exposed to salt fog environment.

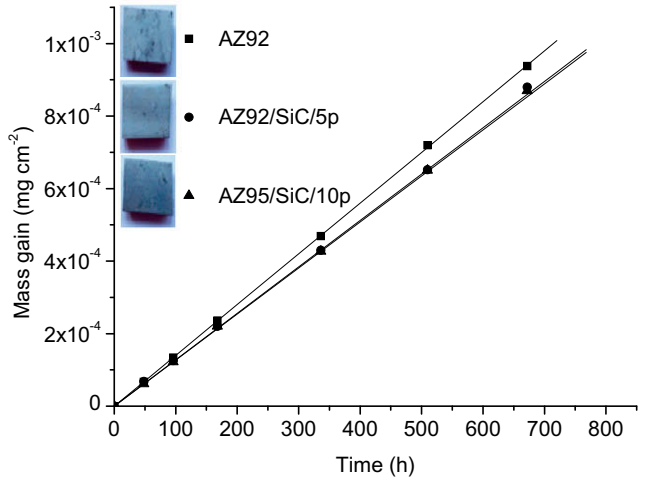

Fig. 6. Mass gain vs. immersion time for the materials exposed to high humidity (98% RH at 50 °C) environment.

orders of magnitude. The addition of SiCp slightly decreased the corrosion rate in this medium. This may be explained by a smaller exposed area of AZ92 magnesium matrix due to the presence of reinforcement and the negligible influence of the SiC particles on the mechanism of corrosion in high humidity environment.

3.5. Morphology and characterization of corrosion products

Fig. 7 shows the surface morphology of tested materials after exposure to salt fog atmosphere for 21 days. The surfaces were covered by a corrosion layer, possibly $Mg(OH)_2$, which was thicker and more uneven in case of the AZ92/SiCp composite materials. Examination of the surface of AZ92/SiC/0-10p materials after exposure to high humidity environment for 28 days revealed an insignificant degree of corrosion with only few corrosion products on the surface (Fig. 8).

Fig. 9 discloses the backscattered electron micrographs of the cross-sections of the AZ92, AZ92/SiC/5p and AZ92/SiC/10p materials after 21 days of exposure to salt fog atmosphere. The corrosion layers were thick and cracked, with incorporation of SiCp in the case of composite materials. The high thickness of the corrosion

Table 2
Kinetic laws of materials exposed to salt fog and high humidity environments.

Material	Kinetic Laws $y = b \cdot t$; [y(mg cm^{-2}), t(h)]			
	Salt Fog		High humidity	
AZ92	$y = 2.50 \times 10^{-4}\ t$	$0 \leqslant t \leqslant 336$ $r^2 = 0.998$	$y = 1.40 \times 10^{-6}\ t$	$0 \leqslant t \leqslant 672$ $r^2 = 0.996$
AZ92/SiC/5p	$y = 9.37 \times 10^{-4}\ t$	$0 \leqslant t \leqslant 168$ $r^2 = 0.964$	$y = 1.28 \times 10^{-6}\ t$	$0 \leqslant t \leqslant 672$ $r^2 = 0.998$
AZ92/SiC/10p	$y = 1.19 \times 10^{-3}\ t$	$0 \leqslant t \leqslant 96$ $r^2 = 0.958$	$y = 1.27 \times 10^{-6}\ t$	$0 \leqslant t \leqslant 672$ $r^2 = 0.998$

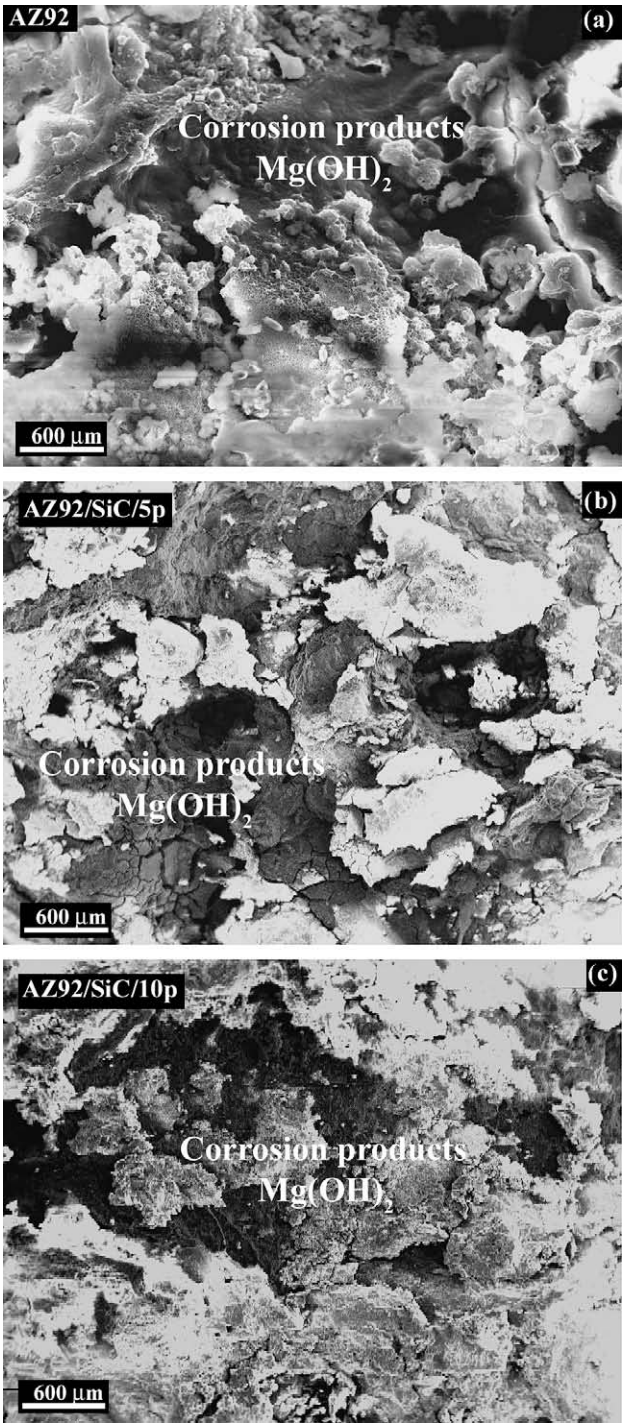

Fig. 7. SEM micrographs of the tested materials surface after 21 days of exposure to salt fog atmosphere.

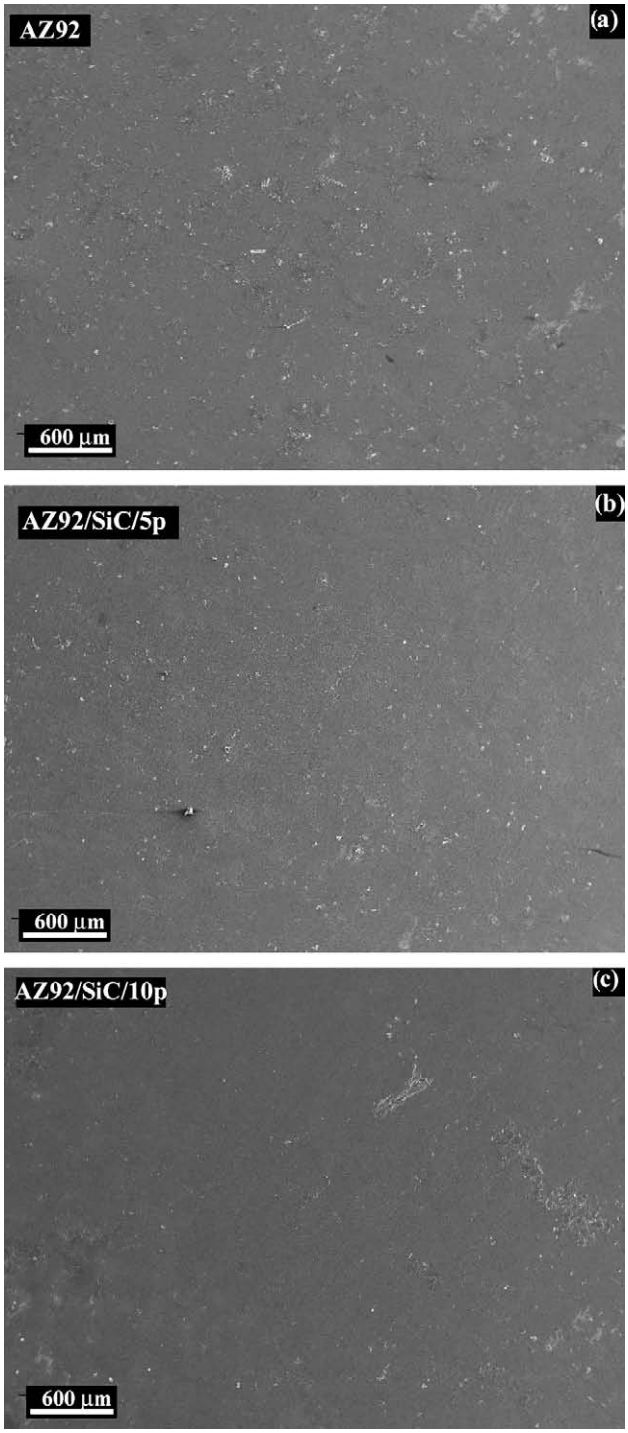

Fig. 8. SEM micrographs of the tested materials surface after 28 days of exposure to high humidity environment (98% RH at 50 °C).

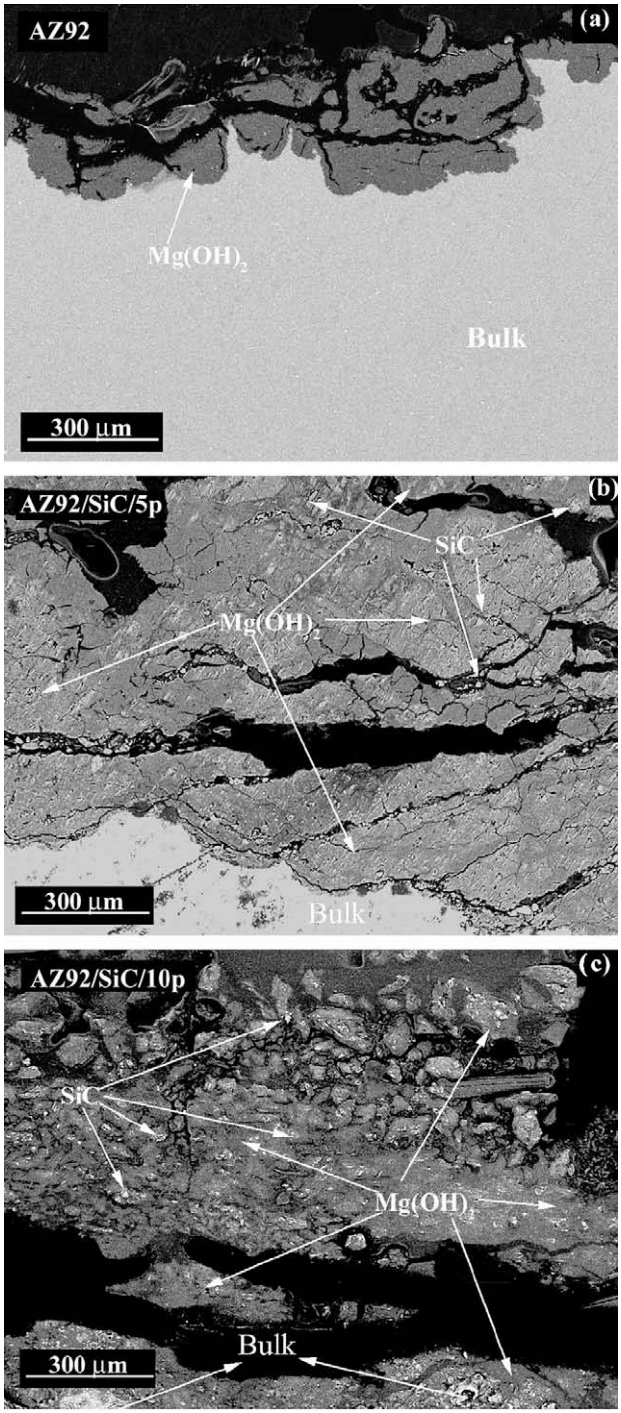

Fig. 9. SEM micrographs of the cross-sections of tested materials after 21 days of exposure to salt fog atmosphere.

layer and the presence of SiCp generated stresses and the subsequent cracking and spalling of these layers as gravimetric measurements suggested. Cracking and spalling processes provide ready access of water, chloride ions and oxygen towards the metallic substrate and continuation of an autocatalytic corrosion process of moderate intensity.

Scanning electron micrographs of the cross-sections of tested materials after exposure to high humidity atmosphere for 28 days revealed almost negligible corrosion of the AZ92 magnesium-based materials (Fig. 10).

The thicknesses of the corrosion layers formed on the tested materials are presented in Fig. 11. Thickness values were the average of 20 measurements from examination of cross-sections by SEM. For salt fog specimens, the spalling of the corrosion products was not considered; therefore it is likely that the real thickness of the corrosion layer was greater than the presented values. In saline environment, the addition of SiCp increased the thickness of the corrosion layer by approximately 2–3 times compared with the unreinforced AZ92 magnesium alloy. When the materials were exposed to the high humidity environment the thicknesses of the corrosion layers were reduced by three orders of magnitude.

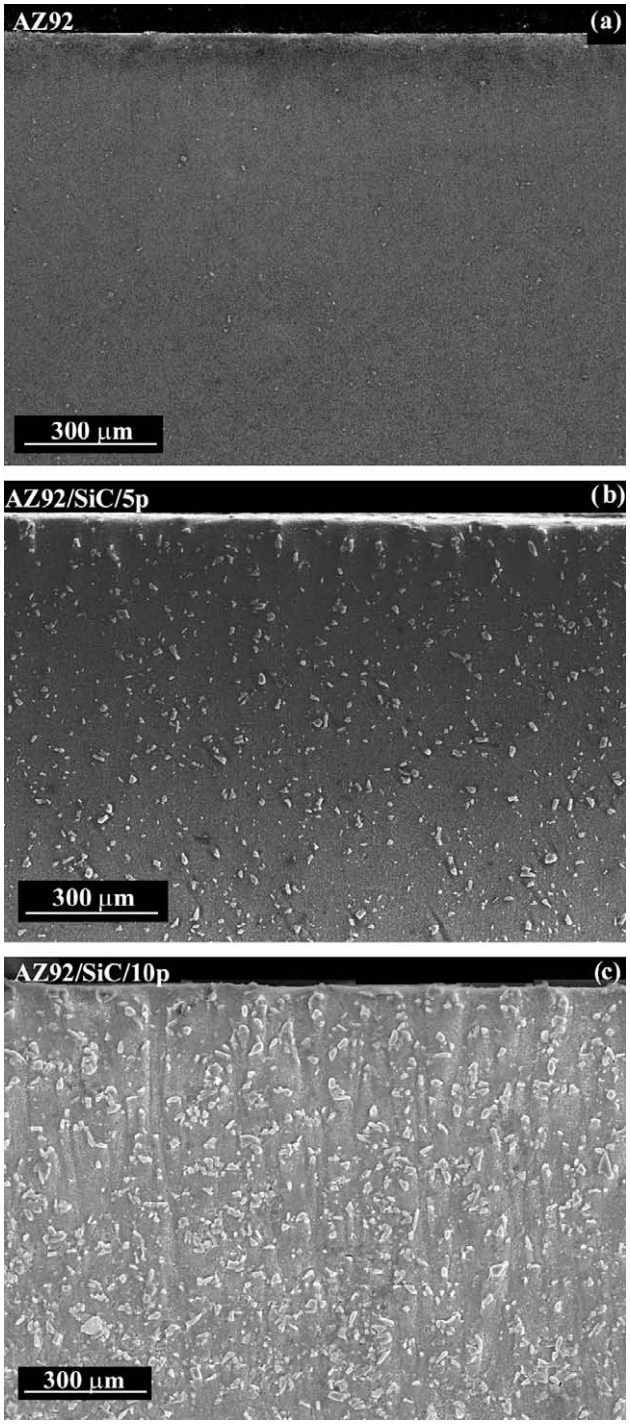

Fig. 10. SEM micrographs of the cross-sections morphology of tested materials after 28 days of exposure to high humidity environment (98% RH at 50 °C).

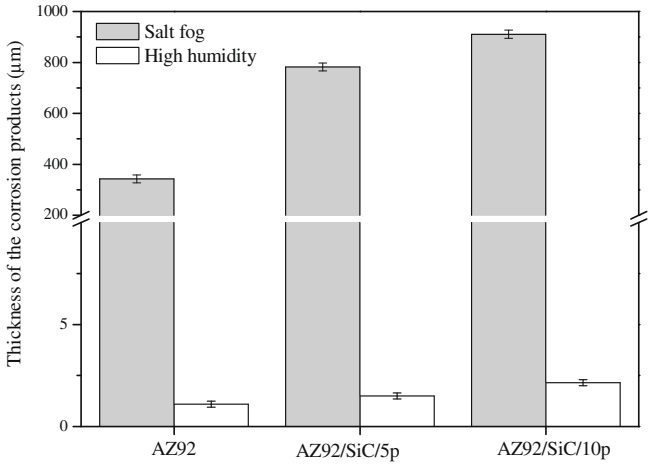

Fig. 11. Thickness of the corrosion layer for the tested materials exposed to salt fog (21 days) and high humidity (28 days) environments.

Fig. 12 reveals the cross-section of the AZ92/SiC/5p composite material and the elemental X-ray maps of magnesium and oxygen after exposure to salt fog for 21 days. According to the elemental maps the corrosion layer mainly consisted of magnesium oxides or hydroxides, possibly $Mg(OH)_2$. Conversely, analogous examination of the same material after exposure to high humidity atmosphere for 28 days revealed very low corrosion susceptibility (Fig. 13).

Higher magnification details of the morphology of corrosion attack in the AZ92/SiC/5p composite exposed to the tested media are shown in Fig. 14. After immersion in 3.5 wt.% NaCl for 1 h, localized corrosion was observed adjacent to the SiC particles, $Mg_{17}Al_{12}$ phase and Al_8Mn_5 inclusions. Similarly, the presence of reinforcement facilitated localized corrosion in salt fog environment. This was manifested by the appearance of corrosion pits and undermined particles. Even though the level of corrosion was not significant in 98% RH at 50 °C, preferential corrosion was observed at the Mg matrix/SiCp interfaces after 28 days of exposure.

Fig. 15a discloses the low angle XRD (incident angle 1°) study of investigated materials after exposure to salt fog environment for 21 days. The results revealed $Mg(OH)_2$ and $(Mg,Al)_x(OH)_y$ as the main corrosion products. The latter revealed lower intensity peaks for the composite materials, suggesting preferential corrosion of magnesium compared with aluminium. On the other hand, XRD measurements following exposure to 98% RH and 50 °C only revealed substrate constituents, confirming the high corrosion resistance of AZ92 composite materials in high humidity atmosphere (Fig. 15b).

4. Discussion

Findings of the present study revealed that the corrosion behaviour of AZ92/SiCp magnesium composite materials was greatly influenced by the nature of the aggressive media. In chloride-containing media, the AZ92 magnesium-based materials revealed severe corrosion attack with formation of corrosion products consisting of $Mg(OH)_2$ and $(Mg,Al)_x(OH)_y$, whereas all the materials revealed higher corrosion resistance after exposure to high humidity atmosphere for 28 days. It is known that Cl^- ions facilitate the formation of a surface electrolyte layer with high conductivity which couples the spatially separated anodic and cathodic processes in the microgalvanic elements on the surface [16]. Thus, the presence of this layer may explain the higher corrosion rate of AZ92/SiCp composites in 3.5 wt.% NaCl and salt fog compared with the high humidity atmosphere. For instance, preferential corrosion was observed at the matrix/Al_8Mn_5 and matrix/$Mg_{17}Al_{12}$ interfaces after exposure to chloride-containing media (Fig. 14).

Regarding the influence of SiCp reinforcement, even though it is an insulator and no galvanic interaction is expected with the AZ92 matrix, it increased the corrosion rate in 3.5 wt.% NaCl aqueous solution and salt fog environment due to the presence of Mg matrix/SiCp interfaces breaking the continuity of the Mg matrix. Also, cracking and spalling of the corrosion layer was revealed for AZ92/SiCp composites after long exposure times in salt fog environment, in particular for the AZ92/SiC/10p material with a higher SiCp volume fraction. On the other hand, in high humidity environment, the influence of the reinforcement was negligible,

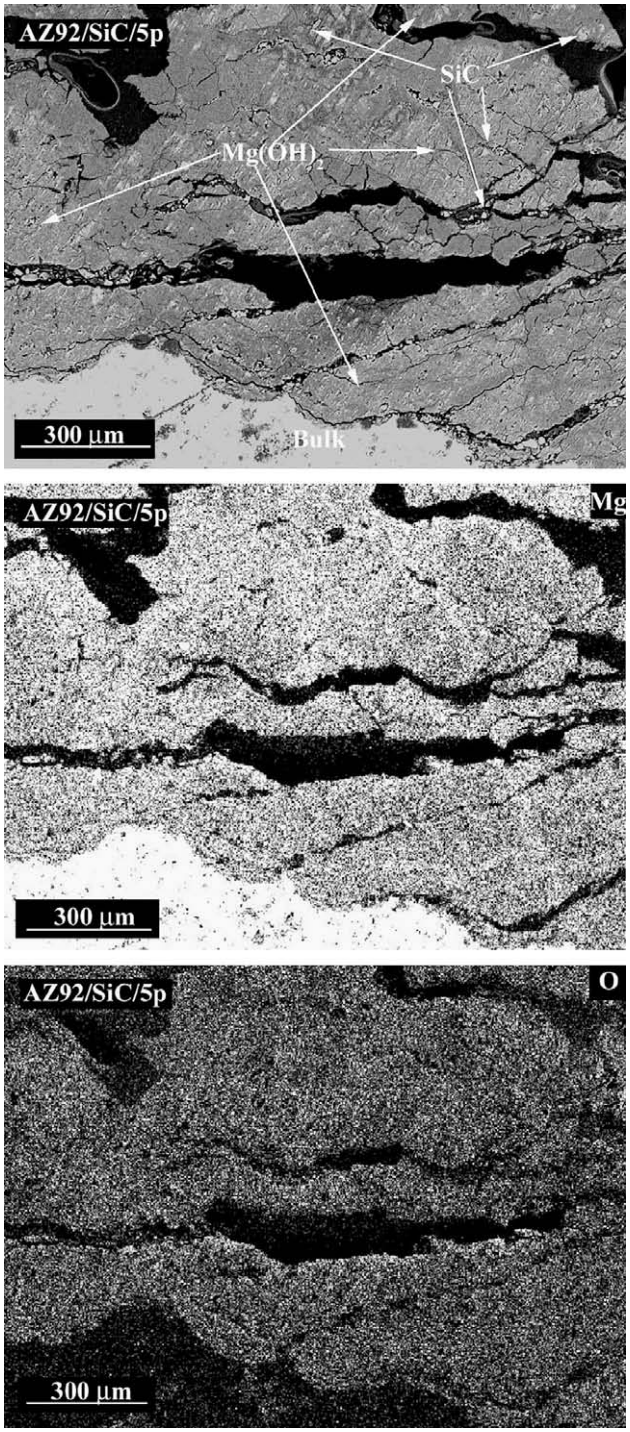

Fig. 12. SEM cross-section micrograph and X-ray elemental maps of Mg and O of AZ92/SiC/5p composite after exposure to salt fog atmosphere for 21 days.

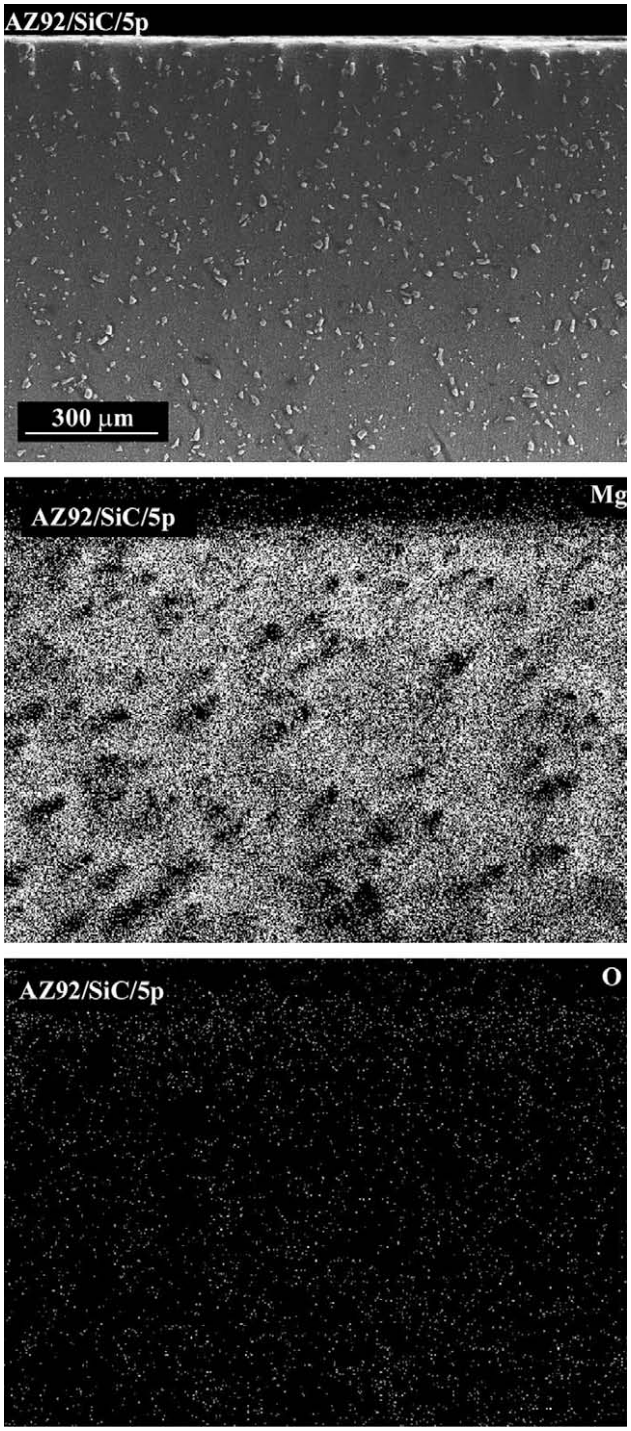

Fig. 13. SEM cross-section micrograph and X-ray elemental maps of Mg and O of AZ92/SiC/5p composite after 28 days of exposure to high humidity environment (98% RH at 50 °C).

although some localized corrosion was observed at the Mg matrix/SiCp interfaces after 28 days of exposure.

5. Conclusions

1. AZ92/SiC/0-10p materials manufactured by powder metallurgy route revealed severe corrosion in salt fog environment with formation of an uneven, cracked and low protective corrosion layer mainly consisting of $Mg(OH)_2$ and $(Mg,Al)_x(OH)_y$ in lower amount. The addition of SiCp increased the degree of corrosion and promoted cracking and spalling of the corrosion layer for increasing exposure times.
2. AZ92/SiCp composite materials disclosed higher corrosion resistance in high humidity atmosphere (98% RH and 50 °C) with almost no influence of SiCp addition on the corrosion behaviour.

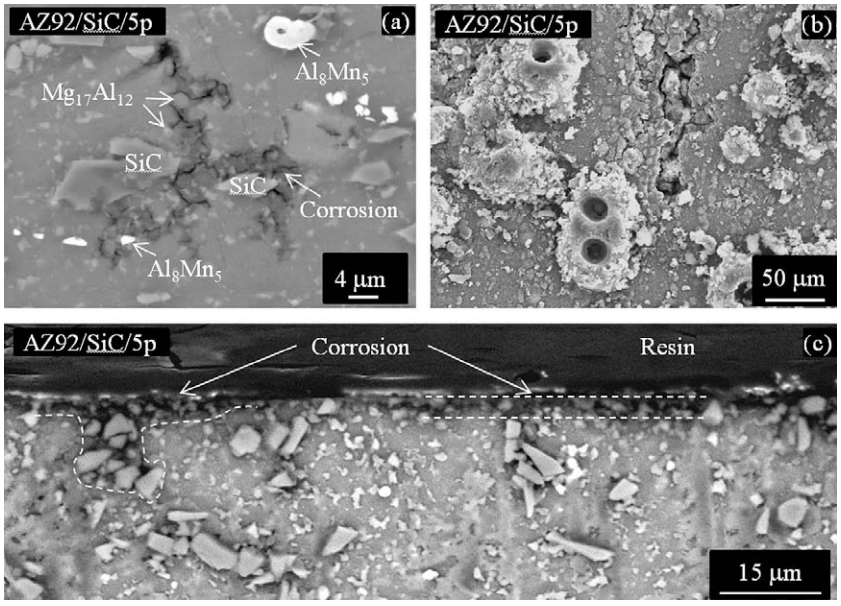

Fig. 14. SEM micrographs of the morphology of the corrosion attack in the AZ92/SiC/5p composite after exposure to (a) 3.5 wt.% NaCl for 1 h, (b) salt fog for 48 h and (c) 98% RH at 50 °C for 28 days.

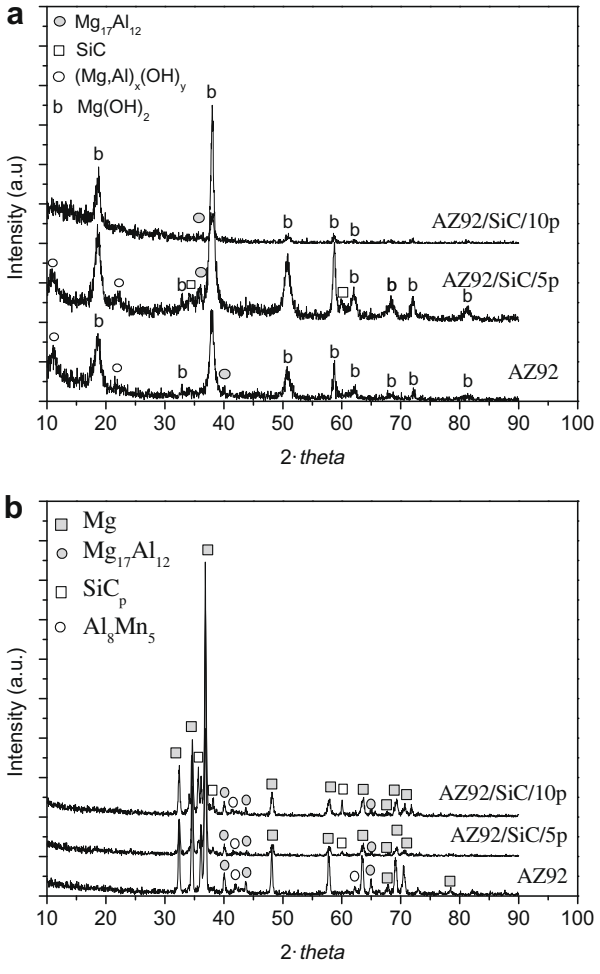

Fig. 15. Low angle XRD (incident angle 1°) study of tested materials: (a) exposed to a salt fog environment for 21 days and (b) to a high humidity environment (98% RH at 50 °C) for 28 days.

3. The morphology of corrosion attack in chloride-containing media revealed localized corrosion at the matrix/$Mg_{17}Al_{12}$ and matrix/Al_8Mn_5 interfaces. This was possibly facilitated by the presence of a surface electrolyte layer with high conductivity which couples the spatially separated anodic and cathodic processes in the microgalvanic elements on the surface. Additionally, localized corrosion was also observed at the matrix/SiCp interfaces, which was possibly due to the reinforcement interrupting the continuity of the magnesium matrix. In high humidity atmosphere, localized corrosion was also observed at these interfaces, however its significance was inconsequential according to the corrosion rate values.

Acknowledgements

The authors are grateful to the MCYT (Project MAT 2006-13179-C02-02), the Community of Madrid (ESTRUMAT_CM MAT/77) for support of this work and also to the MANOEQ of Departamento de Metalurgia Física of CENIM (CSIC) for supply of the composite materials.

References

[1] H.Z. Ye, X.Y. Liu, Microstructure and tensile properties of Ti6Al4V/AM60B magnesium matrix composite, J. Alloys Comp. 402 (2005) 162.
[2] H. Lianxi, W. Erde, Fabrication and mechanical properties of SiCw/ZK51A magnesium matrix composite by two-step squeeze casting, Mat. Sci. Eng. A A278 (2000) 267.
[3] M.J. Koczak, S.C. Khatri, J.E. Allison, M.G. Bader, in: S. Suresh, A. Mortensen, A. Needleman (Eds.), Fundamentals of Metal–Matrix Composites, Butterworth-Heinemann, Stoneham, USA, 1993, p. 297.
[4] Q.C. Jiang, H.Y. Wang, B.X. Ma, Y. Wang, F. Zhao, Fabrication of B4C particulate reinforced magnesium matrix composite by powder metallurgy, J. Alloys Comp. 386 (2005) 177.
[5] Y. El-Saeid Essa, J. Fernández-Sáez, J.L. Pérez-Castellanos, Some aspects of damage and failure mechanisms at high strain-rate and elevated temperatures of particulate magnesium matrix composites, Composites B 34 (2003) 551.
[6] Y. Cai, M.J. Tan, G.J. Shen, H.Q. Su, Microstructure and heterogeneous nucleation phenomena in cast SiC particles reinforced magnesium composite, Mat. Sci. Eng. A282 (2000) 232.
[7] Z. Xiuuqing, W. Haowei, L. Lihua, M. Naiheng, In situ synthesis method and damping characterization of magnesium matrix composites, Comp. Sci. Tech. 67 (2007) 720.

[8] H.G. Tang, X.F. Ma, W. Zhao, S.G. Cai, B. Zhao, Z.H. Qiao, Modeling and analysis of the electrical resistance measurement of carbon fiber polymer-matrix composites, J. Alloys Comp. 437 (2007) 285.
[9] R. Zeng, J. Zhang, W. Huang, W. Dietzel, K.U. Kainer, C. Blawert, W. Ke, Review of studies on corrosion of magnesium alloys, Trans. Nonf. Metals Soc. China 16 (2006) s763.
[10] A. Pardo, M.C. Merino, A.E. Coy, R. Arrabal, F. Viejo, E. Matykina, Corrosion behaviour of magnesium/aluminium alloys in 3.5 wt.% NaCl, Corros. Sci. 50 (2008) 823.
[11] M. Jönsson, D. Persson, D. Thierry, Corrosion product formation during NaCl induced atmospheric corrosion of magnesium alloy AZ91D, Corros. Sci. 49 (2007) 1540.
[12] C.A. Nunez-Lopez, H. Habazaki, P. Skeldon, G.E. Thompson, H. Karimzadeh, P. Lyon, T.E. Wilks, An investigation of microgalvanic corrosion using a model magnesium-silicon carbide metal matrix composite, Corr. Sci. 38 (1996) 1721.
[13] S. Tiwari, R. Balasubramaniam, M. Gupta, Corrosion behavior of SiC reinforced magnesium composites, Corros. Sci. 49 (2007) 711.
[14] Y.Q. Wang, M.Y. Zheng, K. Wu, Microarc oxidation coating formed on SiCw/AZ91 magnesium matrix composite and its corrosion resistance, Mater. Lett. 59 (2005) 1727.
[15] G. Song, S. Hapugoda, D. St. John, Degradation of the surface appearance of magnesium and its alloys in simulated atmospheric environments, Corros. Sci. 49 (2007) 1245.
[16] R. Lindström, L.G. Johansson, G.E. Thompson, P. Skeldon, J.E. Svensson, Corrosion of magnesium in humid air, Corros. Sci. 46 (2004) 1141.
[17] L. Cui, L. Xiaogang, Role of CO_2 in the initial stage of atmospheric corrosion of AZ91 magnesium alloy in the presence of NaCl, Rare Met. 25 (2006) 190.
[18] R. Lindström, L.G. Johansson, J.E. Svensson, The influence of NaCl and CO_2 on the atmospheric corrosion of magnesium alloy AZ91, Mater. Corros. 54 (2003) 587.
[19] R. Lindström, J.E. Svensson, L.G. Johansson, The influence of carbon dioxide on the atmospheric corrosion of some magnesium alloys in the presence of NaCl, J. Electrochem. Soc. 149 (2002) B103.
[20] W.A. Ferrando, Review of corrosion and corrosion control of magnesium alloys and composites, J. Mater. Eng. 11 (1989) 299.
[21] G. Garcés, F. Domínguez, P. Pérez, G. Caruana, P. Adeva, Effect of extrusion temperature on the microstructure and plastic deformation of PM-AZ92, J. Alloys Comp. 422 (2006) 293.
[22] G. Garcés, P. Pérez, P. Adeva, Effect of the extrusion texture on the mechanical behaviour of Mg-SiCp composites, Scripta Mater. 52 (2005) 615.
[23] L.H. Hihara, P.K. Kondepudi, The galvanic corrosion of SiC monofilament/ZE41 Mg metal-matrix composite in 0.5 M $NaNO_3$, Corros. Sci. 34 (1993) 1761.
[24] C.A. Nunez-Lopez, P. Skeldon, G.E. Thompson, P. Lyon, H. Karimzadeh, T.E. Wilks, The corrosion behaviour of Mg alloy ZC71/SiCp metal matrix composite, Corros. Sci. 37 (1995) 689.